Effects of Current and Future Upwelling on Red Abalone (*Haliotis Rufescens)* Larval Development and Survivorship.

Jasmin Juarez-Gonzalez, California State University Monterey Bay

Mentors: Jim Barry and Steve Litvin

Summer 2023

ABSTRACT

Monterey Bay is located within the California Current system where many upwelling ecosystems exist. The high productivity and cold waters of these upwelling regions come with the burden of naturally low oxygen and low pH levels, which periodically expose many nearshore organisms to stressful conditions. These regions are susceptible to climate change, as the dynamic relationship between temperature, dissolved oxygen, and pH can change and create severe conditions for upwelling ecosystems. It is projected that temperatures will increase, while dissolved oxygen and pH levels will continue to decrease and many organisms including sedentary calcifiers will be affected by this change. We wanted to understand the effects of current and future upwelling on red abalone, *Haliotis Rufescens,* larvae in terms of development, survival, and settlement success. Our approach was to rear red abalone larvae in experimental chambers under four different conditions, two of them being variable to simulate upwelling and two average conditions at a constant set point. We had a future variable, a future constant, a current variable, and a current constant treatment. Our results showed a low survival percentage by day six and day 3 of the experiment which various factors within our experimental design may have caused. Looking closer at data from day three, we found some variability between

treatments when examining survival and larval development. This may be due to the larval preference for constant conditions and higher temperatures in the future conditions likely resulting in faster development.

INTRODUCTION

UPWELLING

Monterey Bay is located within the California Current Large Marine Ecosystem (CCLME) where many upwelling ecosystems exist due to being located in an eastern boundary current where strong winds move currents toward the equator. The process behind winds and currents creating an upwelling environment falls to a process known as the Ekman Transport. Winds coming from the North and moving down South create friction on the ocean's surface waters which drive ocean currents out to create the upwelling cycle of warmer waters downwelling into the deep ocean while cold nutrient-rich water is delivered to the nearshore from the deep sea. These upwelled waters contain a dynamic relationship between temperature, dissolved oxygen (DO), and pH whereas the cold nutrient-rich water is naturally low in DO and pH. While they do create a productive environment along the CCLME, they can also provide periodic stressful conditions for many organisms living in this region. The upwelling season happens around the spring and summer months. The oceans can experience diurnal and semidiurnal upwelling where there are relaxation periods with ambient conditions being experienced in the nearshore intertwined with the upwelling events throughout the days (Booth, 2011). These dynamic processes allow for high productivity within this region by introducing cold nutrient-rich waters from the deep sea and also buffering warming effects happening in the nearshore (Lourenço, et al. 2020). Now the persistent issue that the CCLME is facing is climate change and the changing water conditions that come along with it that are foreseen to disrupt many marine ecosystems and deplete productivity. Especially within upwelling regions where they are most vulnerable due to their natural conditions of low oxygen and pH (Reum, et al. 2015).

CLIMATE CHANGE

Anthropogenic activities are raising the amount of carbon dioxide (CO_2) within the atmosphere which allows for the entrapment of greenhouse gasses causing many disbalances in

the climate. We are currently experiencing warmer climates and rising ocean temperatures. The ocean acts as the greatest cooling mechanism for our environment by absorbing excess temperature found in the atmosphere and enabling an increase in temperature in ocean waters. The excess CO_2 emissions are being absorbed into the ocean and raising the carbonate levels leading to lower pH levels and ocean acidification. Climate change introduces a triple threat to our ocean: warmer water, lower DO, and lower pH levels. These conditions are not ideal for many organisms sensitive to temperature differences and fluctuating pH levels, such as calcifiers. These changing conditions enabled by climate change can potentially affect behavior aspects, genomic expression, developmental, breeding, and survivorship of the diverse organisms living in different marine ecosystems (Somero, et al. 2015). However, when focusing on upwelling regions, climate change is projected to alter the dynamics behind the water chemistry during upwelling (Bakun, 1990). Upwelled water will become lower in DO and pH, but also warmer than the current conditions that are being observed. There will be differences in the dynamic relationship between temperature, dissolved oxygen, and pH, with different combinations that organisms have not been exposed to and therefore are not adapted to survive. In this scenario, there is a higher chance of affecting the highly productive ecosystems within upwelling regions (Reum, et al. 2015).

ABALONE

We decided to explore the effects of the chain reaction of climate change affecting upwelling regions by taking a closer look at how red abalone larvae would respond to current and future upwelling patterns. More specifically, we wanted to analyze larval development, survivorship, and settlement under those specific conditions. We chose to use red abalone as our species model for this experiment because they are benthic and sedentary calcifiers, they are broadcast spawners, and they have a relatively short pelagic larval duration(PLD) where no feeding is needed. By using a sedentary calcifying organism we can address the issue of having lower pH levels in upwelling regions and understand how it can potentially affect other calcifiers and other animals living within their threshold environments. Abalone can't escape stressful environments and relocate to habitats with environmental conditions that are less stressful. So, they can be used as proxies to understand what the ecosystem is experiencing as a whole. Also, since abalone are broadcast spawners, we can understand the detrimental consequences that

fertilization, larval recruitment, and larvae development processes for other organisms will suffer from having harmful temperatures, oxygen levels, and pH levels. Lastly, abalone are convenient specimens to conduct experiments on because they have a relatively short PLD which means that lab experiments can be done in a short period when it comes to their larval stages such as our study.

Apart from being proxies, abalone are important to fisheries and their ecosystems as a whole. In their natural environment abalone are kelp grazers and make way for new kelp growth and they compete with sea urchins who are currently overpopulating many kelp forests along the CCLME. Part of the effort to restore abalone populations is having abalone farms which contribute to the fisheries economy and complexity (National Oceanic and Atmospheric Administration). This gives a larger perspective on why scientists are making efforts to study different life stages and components revolving around abalone and why it's important to understand how they will be affected by future conditions enabled by climate change in upwelling regions. There have been other studies focused on different life stages of abalone in general and how the effects of ocean acidification will impact them. It has been found that declining oxygen levels have negligible effects on fertilization success and increasing temperatures mitigate some of the negative effects of low pH, but low pH levels overall were impeding fertilization success (Boch, et al. 2017). The negative effects of low pH also affect larval survivorship and shell calcification, but does not significantly affect settlement (Crim et al 2011, Bryne et al 2010). Increasing temperature also negatively affects shell calcification in red abalone and it contributes to their fast developmental rate; there is a threshold of 18℃ before they start showing signs of mortality (Bryne et al 2010, Leighton, 1974).

Being cognizant of the experimental designs behind most of these studies there was a need to analyze the larval and settlement stages of red abalone in variable conditions rather than constant conditions. Our focus was to study the larval development, survivorship, and settlement success under variable conditions reflecting current and future upwelling to get a deeper understanding of how the dynamic relationship between temperature, DO, and pH would have a combined effect on early developmental stages for the red abalone. Focusing on this particular stage would give us a broader understanding of the effects of climate change on species populations by examining the early life stages that are the building blocks of their survival in the future. Overall our experimental design was tailored to focus on how the effects of climate

change in upwelling regions will have an impact on the early larval development, settlement, and survivorship of red abalone by rearing them under four different conditions: future variable (FV), future constant (FC), current variable (CV), and current constant (CC).

MATERIALS AND METHODS

UPWELLING SYSTEM

Using an upwelling simulator software system created by MBARI engineers we were able to establish 4 different conditions to rear our red abalone larvae (Barry et al. 2017). We chose to have 2 treatments for future conditions and two treatments for current conditions. First, we had FV conditions which simulated a semidiurnal upwelling cycle that went from 6-hour relaxation periods to 6-hour upwelling periods in conditions reflecting predicted changes in temperature, pH, and DO associated with climate change. The second treatment was the average of the FV, which we labeled FC. The average set points for this treatment remained constant throughout the duration of the experiment. The third condition was CV which reflected current temperature, pH, and DO levels being observed in the CCLME. CV had lower temperatures compared to FV but it had higher pH and DO levels. These conditions also fluctuated from 6-hour relaxation periods to 6-hour upwelling periods two times per day. The fourth and final condition was the average of CV which was labeled CC and the parameters remained constant throughout the experiment.

The different set points were achieved by the upwelling simulator software which instructed our equipment to aerate the incoming filtered seawater, add nitrogen and carbon dioxide, as well as heat the water to meet our desired set points. Those set points were scheduled to be reflective of our current oceanic conditions and expected future conditions based on climate change effects on upwelling (Reum, et al. 2015). The set points for FV at the relaxation stage were 16°C for temperature, 7.6mg/L for DO, and 7.8pH (Fig.1). For the upwelling stage, the set points were 12°C, 2 mg/L, and 7.3 for pH (Fig.1). The FC conditions were an average of those 6 set points which were 14.5°C, 7.5mg/L, and 7.6pH (Fig.1). For CV the relaxation set points were 13°C, 8 mg/L, and 8 for pH (Fig.1). The upwelling set points for CV were 9°C, 4 mg/L, and 7.6pH (Fig.1). For CC the set points were an average of the CV set points, 11.5℃, 6.5mg/L, and 7.9 for pH (Fig.1).
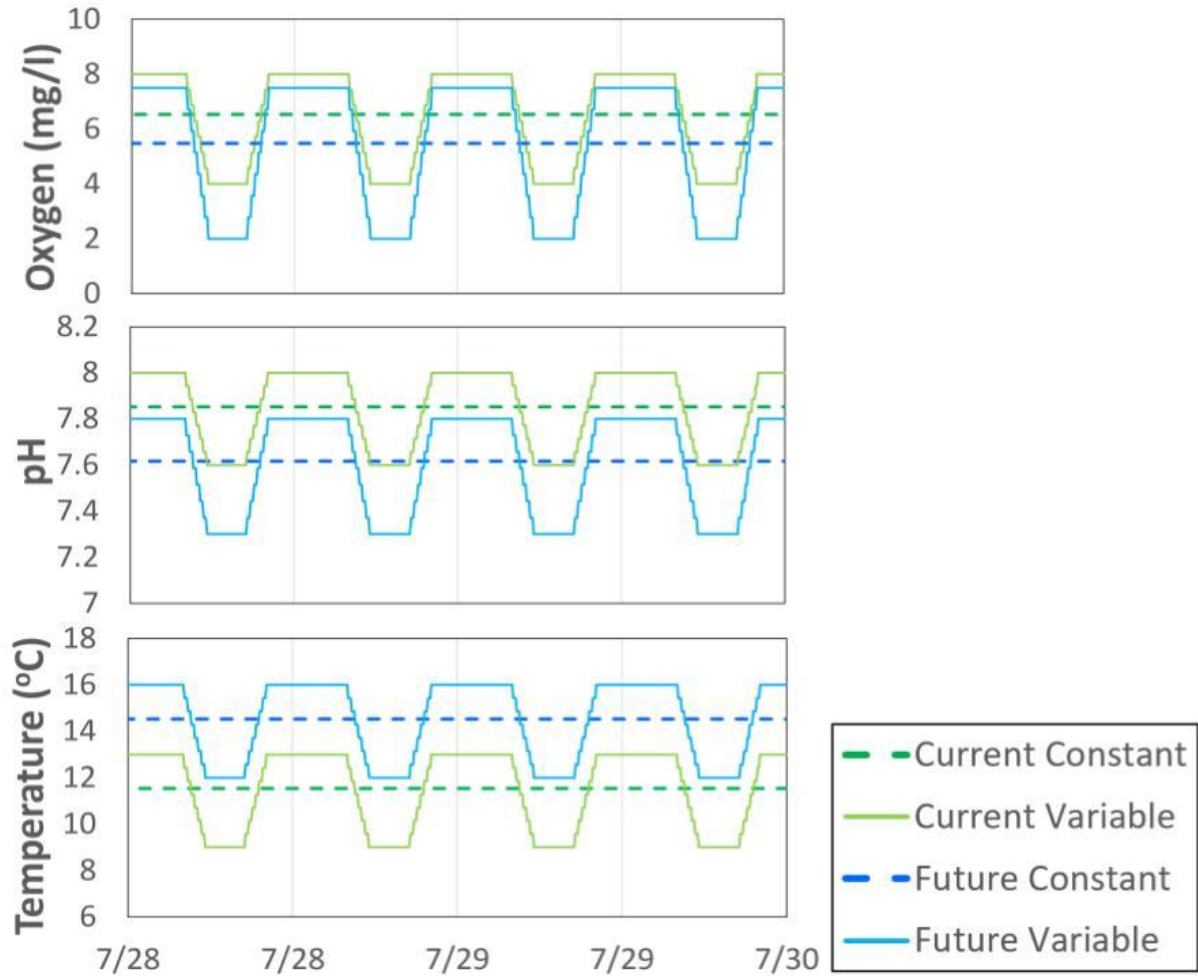
Figure 1: Graph reflects the established set points for the experiment. The x-axis has a total of 2 days plotted to show the semidiurnal upwelling cycle of one day and how it transitions onto the next. The green lines are representative of current conditions; the solid lines depict the variable conditions across DO, pH, and temperature and the dashed lines represent the constant average conditions. The blue lines represent forecasted future conditions, the blue solid line represents the future variable conditions and the blue dashed lines represent the constant average set points across DO, pH, and temperature. **CV**: 9-13°C , 4 mg/L-8 mg/L, 7.6-8 pH. **CC**:11.5°C, 6.5mg/L, 7.9 pH. **FV**: 12-16°C, 2 mg/L-7.6mg/L, 7.3-7.8 pH. **FC:** 14.5℃, 7.5mg/L, 7.6 pH.

In addition to the upwelling system, we designed a system to distribute the treated experimental seawater to the abalone larval-rearing experimental chambers. We had a variety of tanks at different positions with different roles. We had 3 conditioning tanks (CT), 1 reservoir tank (RT), 9 replicate experimental chambers (EC), and 1 sensor chamber (SC) per treatment (Fig.2). In total, we had 12 CTs, 4 RTs, 36 ECs, and 4 SCs. The role of the CTs was to regulate the water chemistry from the incoming filtered seawater. The CTs had multiple sensor probes

taking a reading of the pH, DO, and temperature. The upwelling system software would take that information and instruct the dials inside the CT to add more gasses into the water and or heat the water as well (Barry et al. 2017). The RTs would then receive the water that had reached the programmed set points, these tanks also had sensor probes in them to keep track of the parameters throughout our setup. The water would be pumped out and delivered to the ECs and SCs at 50mL/min. The ECs were the only chambers that contained larvae and the SCs only contained DO probes, pH probes, and temperature probes to understand the water chemistry being experienced at the level of the ECs. Our experimental chambers and sensor chambers were all closely monitored throughout the duration of the experiment.

Figure 2: Diagram of upwelling system set up (left). Image of the complete lab set up with red conditioning tanks at the top, blue reservoir tanks at the bottom back portion of the water table, and the clear experimental tanks along with sensor tanks at front of the water table (center). Close-up images of 9 replicate ECs and examples of SCs with their corresponding sensor probes (right).

EXPERIMENTAL CHAMBER BUILDING

The materials that were used for the ECs and the SCs were clear scratch and UV-resistant acrylic round tubing with an internal diameter of 3.5" and 1⁄8" wall thickness, 80μm Nitex mesh, 1⁄8" to 1⁄8" elbow nozzle connector, 1⁄8" diameter tubing for water delivery lines, clear scratch- and

UV-resistant cast acrylic sheet, 1" plastic bolts, and 1500mL capacity glass beakers with 16.5cm height and an outside diameter of 11.5cm (Fig 3.). We started by cutting 44 pieces of acrylic tubing at 16.5cm for the top portion of our EC where the larvae would be inoculated and then cutting 44 base pieces out of the same material at about 3.5cm in height. We moved on to a process of machine sanding and hand sanding the ends of all 88 pieces of tubing to have flat polished surfaces to glue together. Our next step was to drill (5) $3/4$" diameter holes all spaced at about 6 cm in distance from each other around the base pieces for outflow of the incoming water. After having all 44 bases drilled, the top portions of the chamber and the bases were glued together with 80μm Nitex mesh between them. Using the UV-resistant cast acrylic sheet, the tops of the chambers were water jetted into a circular shape with a 12.3cm diameter to sit on top of the chamber and prevent off-gassing as well as the introduction of foreign objects into the ECs. The tops for the SCs had holes drilled into them to fit each of the sensor probes that would be inserted from the upwelling system. The final step was to drill a $1/8$" hole near the top of the EC to introduce the water delivery line with the ⅛" to ⅛" elbow nozzle. The chambers that were built were then placed in the 1500mL beakers to conserve the water volume within the ECs and SCs(Fig.2). The water height was controlled by the height of the glass beaker and the effective volume within our chambers was about 800mL.

Figure 3: Experimental chambers/Sensor chambers close up.

FERTILIZATION AND REARING PROCESS

After having all the components of the upwelling system and experimental chambers ready we partnered with the Monterey Abalone Company for the spawning and fertilization process. Their broodstock consisted of 3 males and 8 females that were induced to spawn by using a Tris buffer and a hydrogen peroxide (H_2O_2) solution. Buckets of 10L liters were used for the broodstock, 2 buckets for the males, 2 males in one and 1 male in the other, and 4 buckets for the females with 2 females per bucket. Females were induced to spawn first because they take about 2 hours to spawn whereas males take about 1 hour to spawn. An hour after adding the Tris and the H_2O_2 to the females, the males were induced to spawn.

Once successful spawning was achieved, the eggs were washed and rinsed with ambient seawater (11.5℃) before taking a density count. Density counts were taken by collecting 1mL of eggs from the 10L bucket and counting the number of eggs within that milliliter. After getting that number we would multiply it by 1,000 to convert it to eggs per liter and then multiply by 10 to get the amount of eggs within each tub. We followed that procedure three times for each

bucket containing eggs. If the density or amount of eggs within the tub was too high, we diluted the batch of eggs by transferring half of the batch to another tub and adding seawater at 15℃. For the sperm, we sieved it down to get rid of feces and other particles to be able to accurately make a sperm density count and have higher fertilization rates. We calculated the sperm density by using a hemocytometer to determine the volume of sperm that should be added to the 10L of eggs. The gametes were mixed in their respective tubs and allowed for fertilization to take place within 4 minutes.

The batch of eggs that the Monterey Bay Abalone Company gave us for our experiment had about 118,00 eggs. We transported our eggs from Moss Landing Marine Labs over to MBARI and placed them in a water bath running at 15°C to acclimate them. We monitored the eggs for fertilization success by sorting through about 60 eggs and determining if they were fertilized. The percent success fertilization from that batch of eggs was about 80%. We waited for 6 hours after fertilization until the eggs reached the 8 or more cell stage before taking an egg density count and inoculating them into the experimental chambers. From our total volume of 5L, we concentrated our eggs into 400mL from where we later took 5 samples of 100 microliters and counted the number of eggs in those samples (both fertilized and unfertilized) and took the average which led us to have a density of 530 eggs per milliliter. By having 80% fertilization success we planned to inoculate about 1,250 eggs per chamber to have a final density of about 1.5 larvae/mL within our experimental chambers. Based on our calculations we pipetted 2.36mL into the experimental chambers across all four treatments. To prevent thermal shock and instant mortality the inoculation process included changing the set points to the conditions the eggs were exposed to during development. Those included a temperature of about 15°C and ambient pH and DO. After a few minutes of introducing the eggs to the chambers. We started the upwelling schedule and all parameters slowly moved to their respective set points.

Throughout the experiment, we checked that flows were running into all chambers and we monitored the upwelling system by performing pH spot checks. We also gently stirred the larvae within the experimental chambers with a stirring rod to allow them to swim up in the water column if they were pinned down on the mesh. We made sure to rinse the stirring rod with the treatment water into the respective chamber to ensure no larvae were stuck on it before introducing the rod into a new chamber. We removed foreign debris coming in from the water lines by using a flat-tip tweezer and ensuring not to scrape and tear the mesh. We also performed

a thorough rinse of the tweezers into the chamber to ensure no larvae were taken away from their chambers. We had our remaining eggs in a sieve sitting in a water bath with ambient parameters. We would occasionally take small samples from those to look under the microscope and estimate what stages our experimental larvae would be in.

SAMPLING PROCESS

Water samples were the first to be collected before initiating the experiment to measure the carbonate chemistry present in the water. We had also planned to take samples at the end of the experiment, but we only sampled before beginning the experiment. The procedure consisted of filling a 500mL glass flask with the treatment water. In total, we had 5 flasks, one for each treatment (FV, FC, CC, CV) and one for ambient water. When filling the flasks with the treatment water we were cautious about not introducing air bubbles and leaving enough head space to add the mercuric chloride ($HgCl_2$) and seal the flask. After getting our water sample into the flask we pipetted 200µL of $HgCl_2$ into the flask to "poison the water". We then greased the top stopper cap to seal the flask and store it away. We did not examine the samples within the time we had set for the experiment, but we had the samples ready in case there was a need to know about the water's carbonate chemistry.

Spot checks were conducted at least every 2 days to ensure that the sensors connected to the upwelling system were giving accurate readings. To do this we mainly checked for pH by calibrating a pH probe using two different buffer solutions, one with low pH and another with high pH. The calibrated probe was then inserted into the control tanks and we would compare the reading from the upwelling system to the calibrated probe. From the CTs, we would move on to the reservoir tanks and compare the readings between the calibrated probe and the upwelling system. From there we would move down to the sensor chambers which reflected the water conditions within the ECs. All of those different readings and comparisons were taken from all four different treatments and their set of tanks. The differences between the numbers would be taken into consideration when adjusting offsets in the upwelling system and understanding what the larvae were experiencing. Temperature and DO were routinely meeting their set points and not showing any problems, so they were not monitored as much as pH.

Our sampling days for larvae were set to be on days 3, 6, and 9 of the experiment, and 3 chambers from each treatment were randomly sacrificed per sampling day. To get started we

labeled the 20mL preservation vials with the treatment and the chamber number. We also prepared a 5% formalin solution to preserve our larvae samples. We first disconnected the 3 randomly selected experimental chambers from the water line for the specific treatment. We then took the chamber and rinsed the larvae into the chamber's corresponding beaker making sure to get the larvae off of the mesh and off of the side walls of the chamber. We then poured the larvae from the beaker into a small sieve where we concentrated all the larvae on the edge of the sieve. This made it easier to transfer the larvae into the preservation vials while also using less formalin to rinse the larvae off of the sieve. To complete that transfer step, we placed a funnel on top of the vial and we used a squirt bottle containing formalin to rinse off the larvae from the sieve into the funnel. We were cautious about using less than 20mL of formalin for each vial so that the sample would not overflow. This procedure was repeated for each chamber from each treatment and for each sampling day. After collecting our samples from days 3 and 6 we were ready to take them to analyze under the microscope to score their development and check on the mortality rates per treatment.

DEVELOPMENT SCORING AND SURVIVORSHIP

The samples that were analyzed first were samples from day 6. We wanted to observe if the larvae were getting closer to the competency-to-settle stage. Then after sorting through day 6 samples, we moved on to sampling all samples from FC, one sample from FV, CC, and CV from day 3. The procedure for sorting through the samples was to take a 1mL glass pipette and extract subsamples from the vial and into a 6-well cell culture plate plastic petri dish. Once we had a subsample in each of the 6 wells of the plate it would be taken under the dissecting microscope to take a closer look at the larvae. We used a count clicker to count the number of live larvae both with shell and no shell. A note would be taken of how many had a shell and how many did not have a shell. Along with counting the surviving number of larvae, we scored their development stage using the criteria from Hahn's handbook of the culture of abalone (Fig 4). We would keep count of the number of larvae within their respective life stages to better understand where the majority of the sample was in terms of development, but data was presented as stages observed throughout the sample. After sorting through those 6 wells, the sample would be rinsed into a petri dish. This procedure was repeated until the petri dish was close to being full and then the sample would get rinsed with formalin into a new vial labeled with the same information as

the original. Or if we had gone through the whole sample, it would get rinsed back into the original vial. This was repeated for every sample that was sorted for development and survivorship.

The number of live larvae that were recorded through sorting was compared to the initial number of larvae that we started with to estimate the survival rate of the larvae. The stages in which the larvae were in were taken as qualitative data to demonstrate differences in development rates between treatments.
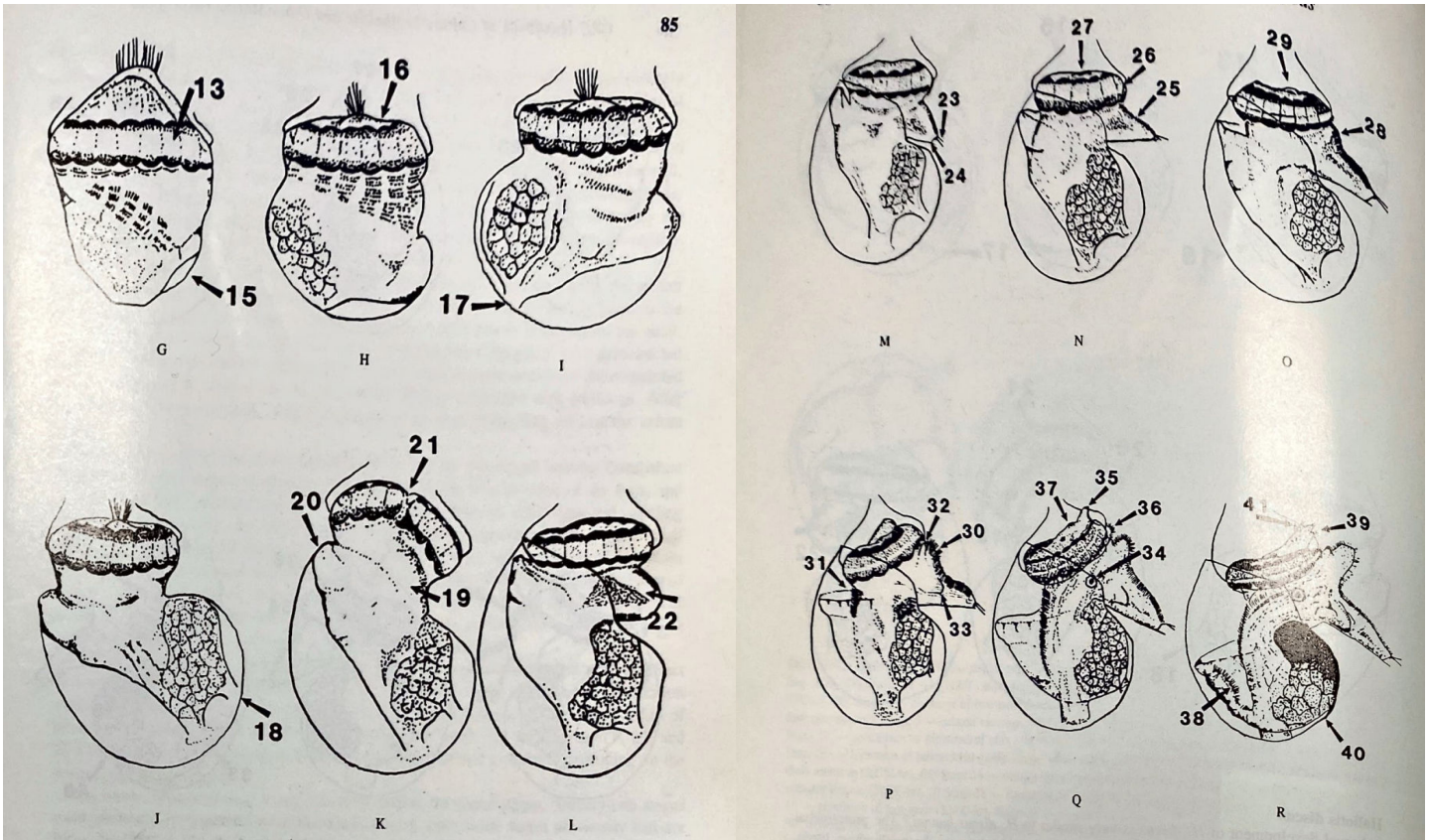

Figure 4: Criteria used for developmental scoring of the red abalone larvae (Hahn 1989). Stage G is the hatch-out stage where they start developing their larval shell, it's considered an early larval stage. The H stage is when the larvae complete their velum. The I stage is when there's an appearance of the retractor muscle. During the J stage, there is the appearance of the integumental attachment to the shell. K stage is when the protrusion of the foot mass is visible and there is the completion of the larval shell along with torsion. The M stage is the formation of the operculum and spines at the end of the metapodium. The N stage is when the eye spot becomes visible. O stage has the formation of the propodium and cephalic tentacles. P stage has cilia growth on the propodium and cilia on the mantle cavity. Finally, stage R is when larvae are competent to settle.

SETTLEMENT

Inducing settlement was programmed to happen on day 8 of the experiment to the sample on day 9, but we did not induce settlement based on our results from the samples that had been collected and sorted. The plan was to transfer the larvae from the experimental chambers into a 960mL glass jar using their treatment water. For both variable conditions, we were going to wait for the period where the parameters were transitioning from an upwelling cycle into a relaxation cycle to be able to target average conditions from those treatments. The jars were going to be filled to a specific water level to have enough space to introduce our GABA solution. After introducing the GABA we were going to seal shut the jars and set them into a water bath to control the temperature of the water. Then they were going to sit in the water bath for about 12 hours and be taken for sampling.

At this point, we were only going to have three jars per treatment and we were going to sample for final survivorship and if the larvae settled. To do that we were going to pour out all the swimming larvae from the settlement jar and those were going to be considered the "non-settlers". The larvae leftover inside the settlement jars were going to be considered "settlers". We were going to dislodge and rinse them from the glass jar by using 70% ethanol to be able to count them and see if many were successful enough to settle. This sample from day 9 was also going to be scored on their development stage using the same criteria used for day 3 and 6 samples.

RESULTS

SURVIVORSHIP

Survivorship on day 3 of the experiment was lower than the 50% minimum that was expected. The percentage of survivorship was at 14% and mortality was at 86% (Fig 5). We obtained these numbers by comparing the average number of live larvae across the experiment within our samples from day 3 and compared it to the initial amount of eggs inoculated at the start of the experiment (Table 1). The current constant conditions had the most live larvae on day 3 and the current variable conditions had the least live larvae (Fig.6). Future constant conditions followed the current variable conditions with low mortality and the future variable conditions had about half the number of live larvae than current constant conditions(Fig.6). By day 3, future

variable had 206 live larvae, FC had 68 live larvae, CC had 449 live larvae, and CV had 51 live larvae (Table 2).
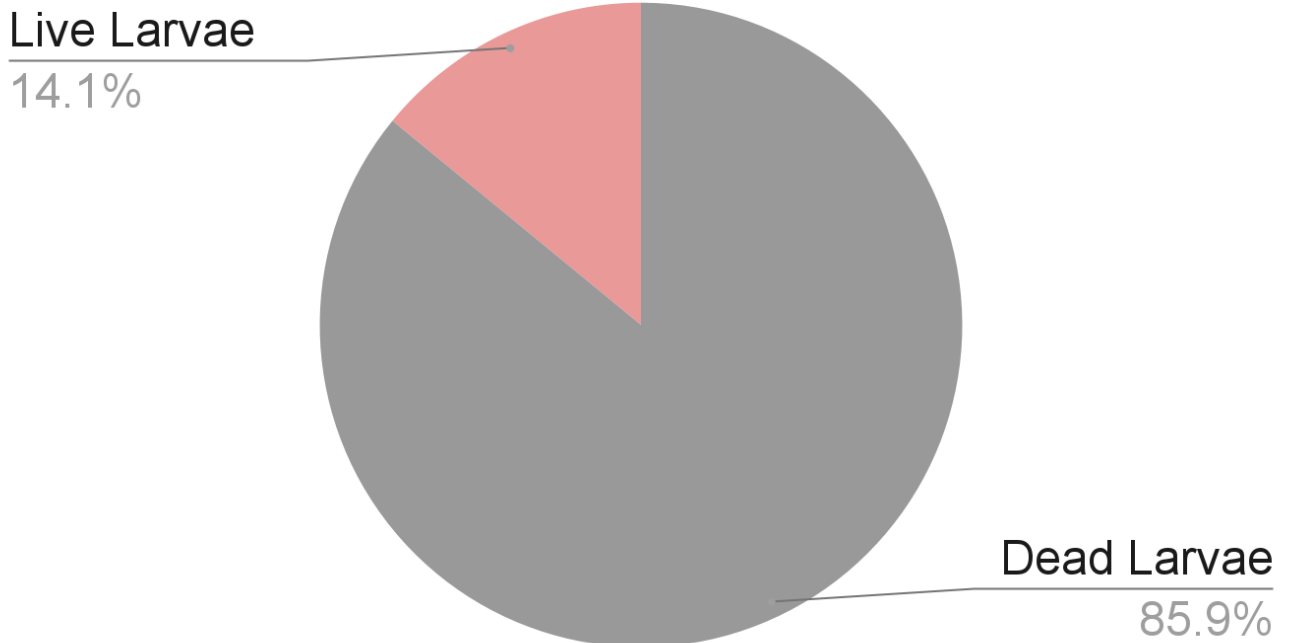

Figure 5: This pie chart shows the percentage of live larvae and dead larvae on day 3. The low survival percentage of 14.1% is shown in pink and the high mortality percentage of 85.9% is shown in gray. There were a total of 1250 inoculated eggs at the beginning of the experiment and the number of live larvae was divided by 1250 to obtain the survival percentage. The mortality percentage was obtained in a similar fashion where the number of surviving larvae was subtracted from 1250 and the difference was divided by 1250.

Table 1: The table shows the larvae survivorship at day 3. It contains the number of average live larvae across the experiment which was 176 average live larvae. The dead larvae across the experiment are also shown, which were 1074 dead larvae. Those numbers were used to calculate the percent survivorship and percent mortality across the experiment by dividing the "Average Live Larvae" value by the initial number of inoculated eggs (1250) and also dividing the "Dead Larvae" value by 1250, respectively.

Larvae Survivorship at Day 3	
Average Live Larvae (Across Experiment)	176
Dead Larvae Across Experiment	1074
Percent Mortality	86%
% survival	14%
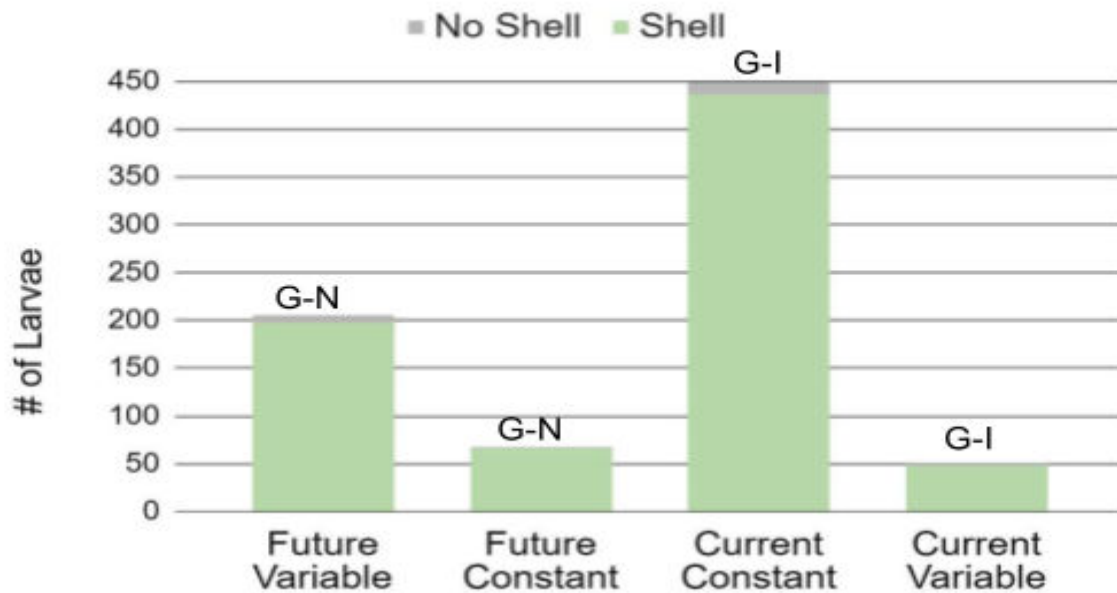
Figure 6: This bar graph shows the number of live larvae within each experimental treatment at day 3. These larvae were categorized as having a shell (in green) or no shell (in gray). The number of larvae is plotted on the y-axis and the 4 different treatments are labeled on the x-axis. At the top of each bar the letters represent the range of developmental stages that were observed within that corresponding experimental condition (refer back to **Fig.4** for descriptions of the letter and indication of developmental stage). FV had a total of 206 live larvae, FC had 68 live larvae, CC had 449 live larvae, and CV had 51 live larvae.

Table 2: This table shows the live larvae across the 4 experimental treatments at day 3. It shows the number of live larvae with a shell and without a shell. The total live larvae are shown in the furthest right column.

Live Larvae Across 4 Experimental Treatments at Day 3			
Experimental Conditions	Shell	No Shell	Total Live
Future Variable (FV)	197	9	206
Future Constant (FC)	66	2	68
Current Constant (CC)	437	12	449
Current Variable (CV)	48	3	51

By day 6 of the experiment survivorship drastically declined down to 2% survivorship and 98% mortality (Fig 7). We also obtained these numbers by comparing the average number of live larvae across the experiment within our samples from day 6 and compared it to the initial amount of eggs inoculated at the start of the experiment. (Table 3). For day 6, the FC conditions had the most live larvae and the CV conditions had the least live larvae (Fig 8). By day 6, FV had 21 live larvae, FC had 39 live larvae, CC had 20 live larvae, and CV had 16 live larvae (Table 4). We did not sample for day 9 due to the high mortality percentage on day 6.
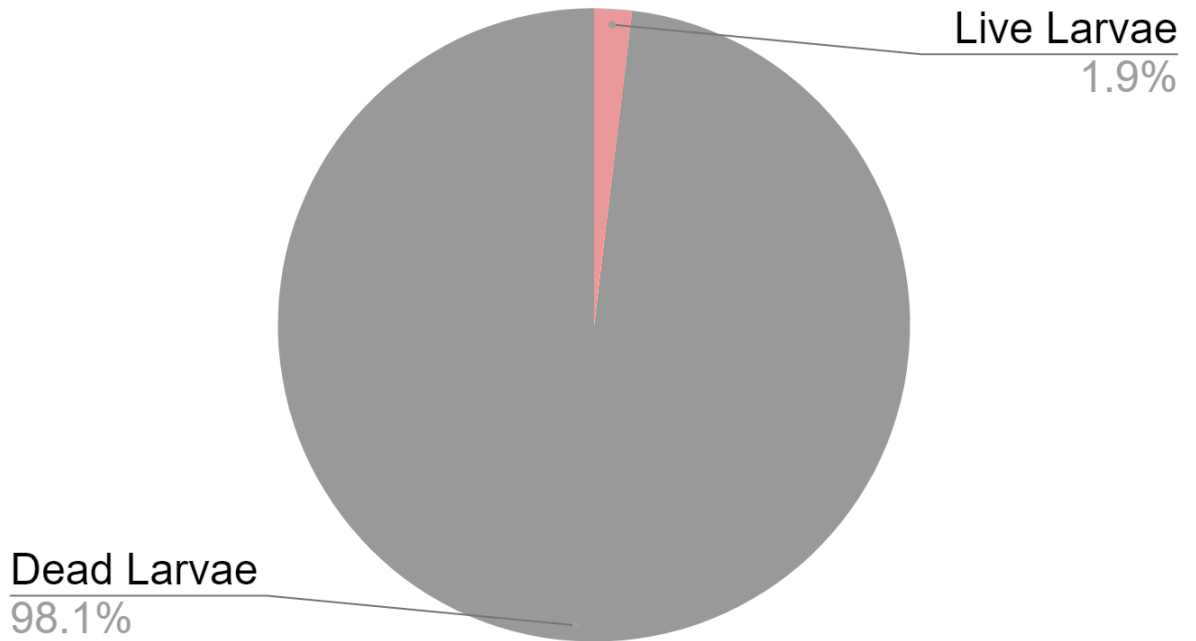
Larvae Survivorship by Day 6

Figure 7: This pie chart shows the percentage of live larvae and dead larvae on day 6. The low survival percentage of 1.9% is shown in pink and the high mortality percentage of 98.1% is shown in gray. There were a total of 1250 inoculated eggs at the beginning of the experiment and the number of live larvae was divided by 1250 to obtain the survival percentage. The mortality percentage was obtained in a similar fashion where the number of surviving larvae was subtracted from 1250 and the difference was divided by 1250.

Table 3: The table shows the larvae survivorship at day 6. It contains the number of average live larvae across the experiment which was 24 average live larvae. The dead larvae across the experiment are also shown, which were 1226 dead larvae. Those numbers were used to calculate the percent survivorship and percent mortality across the experiment by dividing the "Average Live Larvae" value by the initial number of inoculated eggs (1250) and also dividing the "Dead Larvae" value by 1250, respectively.

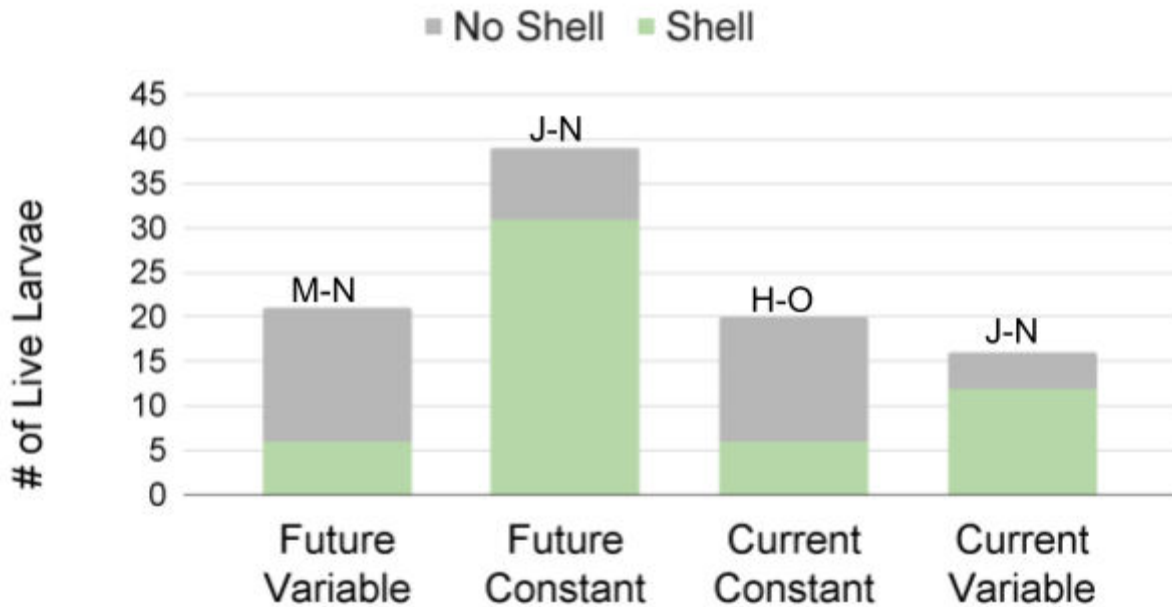| Larvae Survivorship at Day 6	
Average Live Larvae (Across experiment)	24
Dead Larvae (Across experiment)	1226
Percentage of Mortality	98.1%
% survival	1.9%

Live Larvae Sampled from Day 6

Figure 8: This bar graph shows the number of live larvae within each experimental treatment at day 6. These larvae were categorized as having a shell (in green) or no shell (in gray). The number of larvae is plotted on the y-axis and the 4 different treatments are labeled on the x-axis. At the top of each bar the letters represent the range of developmental stages that were observed within that corresponding experimental condition (refer back to **Fig.4** for descriptions of the letter and indication of developmental stage). FV had a total of 21 live larvae, FC had 39 live larvae, CC had 20 live larvae, and CV had 16 live larvae.

Table 4: This table shows the live larvae across the 4 experimental treatments at day 6. It shows the number of live larvae with a shell and without a shell. The total live larvae are shown in the furthest right column.

Live Larvae Across 4 Experimental Treatments at Day 6			
Experimental Conditions	Shell	No Shell	Total Live
Future Variable	6	15	21
Future Constant	31	8	39
Current Constant	6	14	20
Current Variable	12	4	16

DEVELOPMENT

Even though survivorship was persistently low and continuously declining, larval development across the four experimental conditions was advancing. At day 3 across all 4 experimental treatments, the larvae showed characteristics of being in the early larval stage G (Fig 6.). The G stage is the hatch-out and initial development of the larval shell stage (Fig 9). Whereas in day 6 the earliest stage that was observed was the H stage which is when the larvae complete their velum and are ready to move forward to other larval stages (Fig 8). For both current treatments on day 3, the latest developmental stage that the larvae were able to reach was stage I, and on day 6 the latest stage that was observed was stage O which is significantly closer to being competent to settle. The surviving numbers were too low to be able to make an accurate comparison and quantitative analysis, but those were the main observations between the two sampling days.

To an extent, there was variability with development stages across the four treatments at day 3. Both future conditions had their larvae develop until the N stage, which is when the eye spot appears and indicates that it is closer to becoming competent to settle (Fig 9). Both current conditions at day 3 were only able to have their larvae develop until the I stage (Fig 6). Day 6 had less variability between treatments when looking closer at the latest developmental stage that the larvae were able to reach (Fig 8).
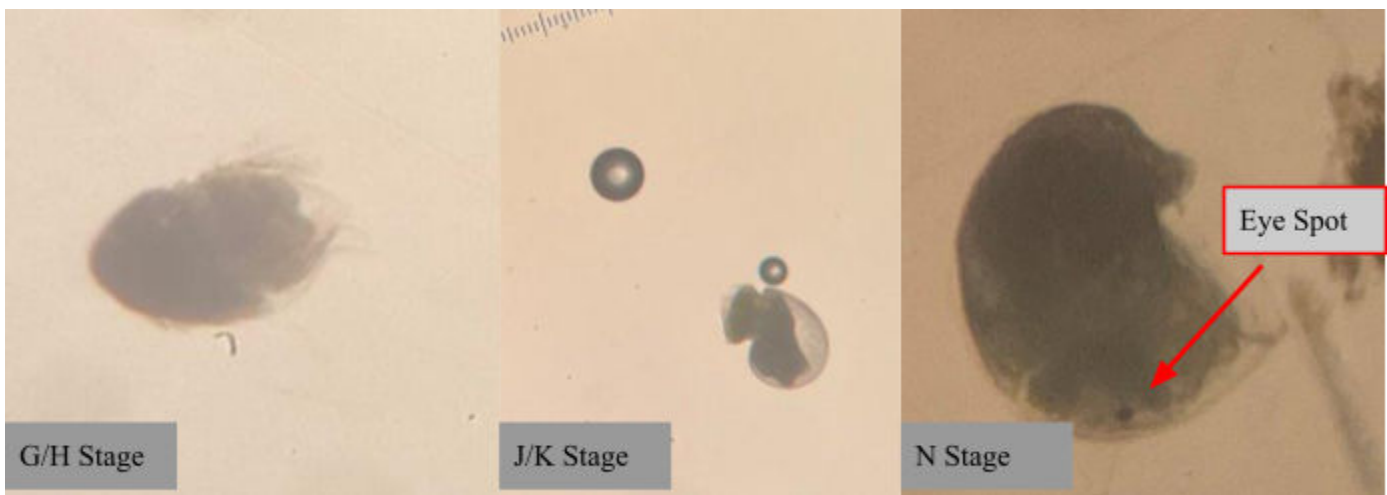

Figure 9: Left side is a larva at the hatching stage and beginning of larval shell development, G/H stage. This stage was observed across all 4 treatments at day 3 and some at day 6. The image at the center shows a larva at the J/K stages which was observed only in the future experimental conditions at day 3 and across all 4 experimental

conditions at day 6. The left image is a larva at the N stage where the eye spot is visible. This stage was only observed in the future experimental conditions on day 3 and across all 4 experimental conditions on day 6.

SETTLEMENT

No results for settlement are available because of the low survival percentage at day 6 (Fig 7).

UPWELLING SYSTEM PERFORMANCE

Throughout the experiment, we monitored the upwelling system and its performance. We found that throughout all the experimental conditions, pH was only meeting the setpoints for a small amount of time. Especially in the FV and CV treatments the pH would meet the set point for either the relaxation or upwelling period for a certain amount of time and then it would surpass or fail to meet the set points (Fig 10). For the constant treatments, FC and CC the same pattern was observed where the pH set point was being met for certain periods of time, but it would surpass or fail to meet the programmed set point values. A similar process occurred with DO levels. The upwelling system demonstrated the ability to follow our programmed upwelling and relaxation cycles within our variable conditions, but the set points for DO were not fully met in those variable treatments. The constant treatment set points were not fully met either for the DO levels. There were fluctuations that were not desired within our constant treatments for both pH and DO (Fig 11). Temperature was the only parameter that had fewer issues with meeting the programmed set points for all experimental conditions. The temperature across all treatments was achieved by our upwelling system and it did not seem to have a problem (Fig 10, Fig 11).
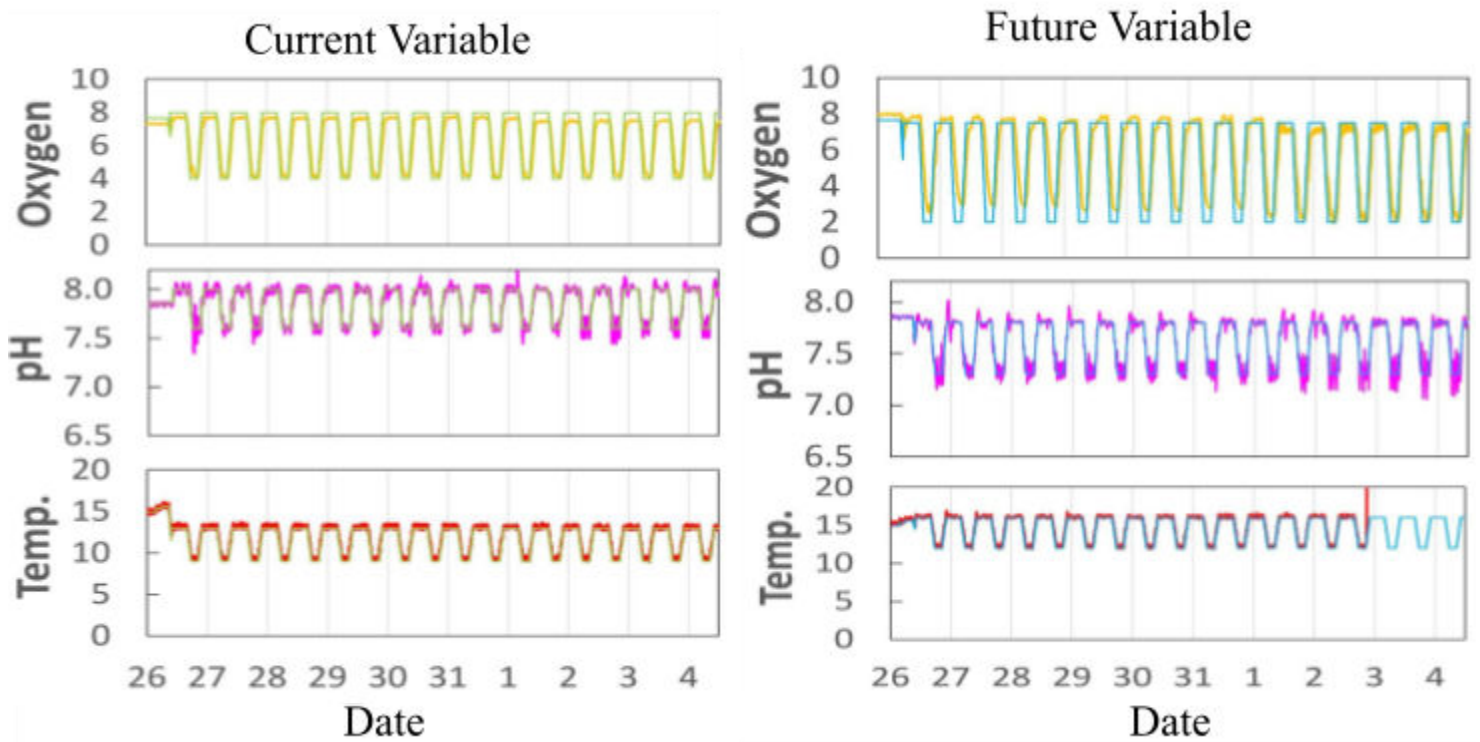
Figure 10: Current variable upwelling system performance is on the left. The solid green lines are the programmed set points for current variable conditions for all three parameters, DO, pH, and temperature. The oxygen performance is at the top shown by the yellow line, the y-axis for oxygen ranges from 0 to 10 to show the DO levels as the upwelling system attempts to reach the set points. The middle graph from top to bottom shows the pH in the pink line, the y-axis for pH ranges from 6.5 to 8.0. Temperature is shown at the bottom graph by the red line while the y-axis ranges from 0 to 20. The x-axis for both current variable and future variable are the dates that range from July 26, 2023, to August 4, 2023. The right side set of graphs represents the performance for future variable. The solid blue lines are the programmed set points for future variable conditions. Oxygen is shown at the top by the yellow line and the y-axis range is from 0 to 10. The pH is in the middle graphs from top to bottom and is shown by the pink line with a y-axis range of 6.5 to 8. Finally, the temperature is at the bottom shown by a red line and a y-axis range of 0 to 20. (spike in temperature in future variable was from a misplaced sensor)
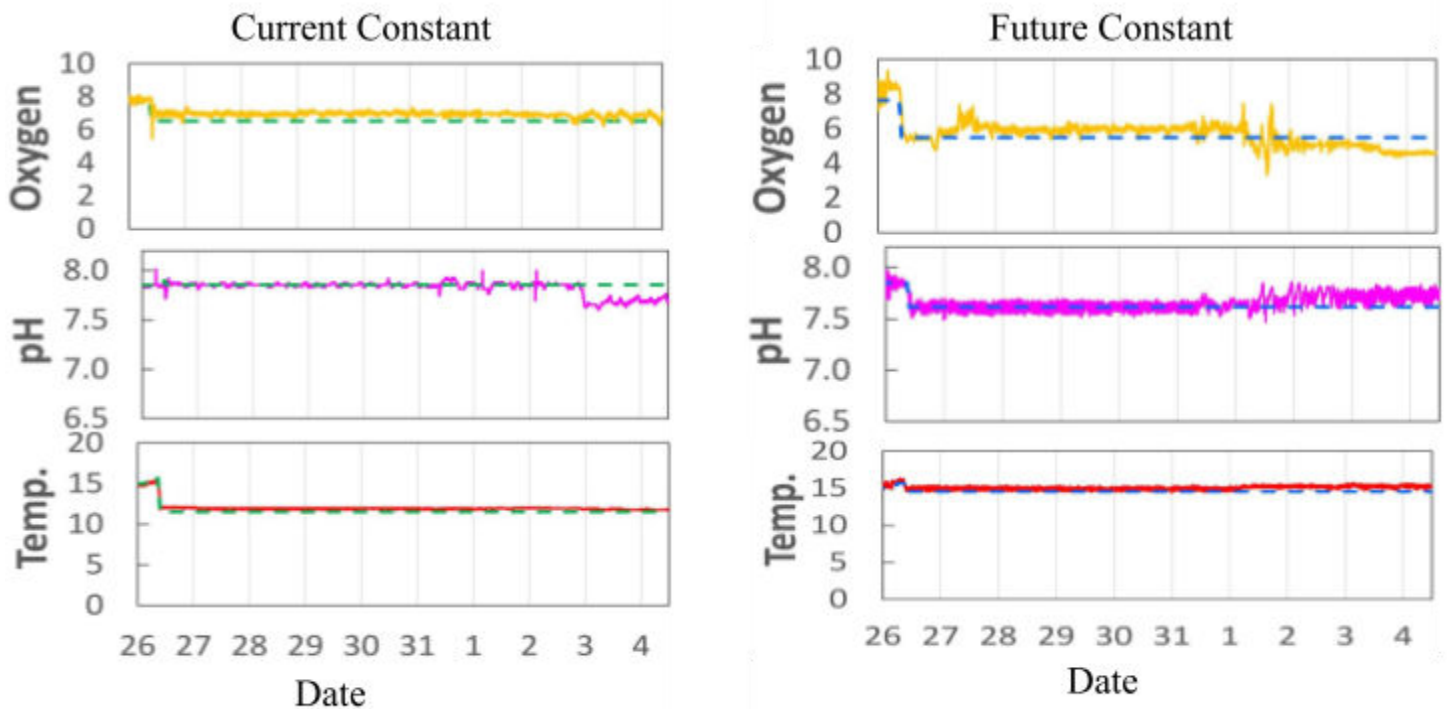
Figure 11: Current constant upwelling system performance is on the left. The dashed green lines are the programmed set points for current variable conditions for all three parameters, DO, pH, and temperature. The oxygen performance is at the top shown by the yellow line, the y-axis for oxygen ranges from 0 to 10. The middle graph from top to bottom shows the pH in the pink line, the y-axis for pH ranges from 6.5 to 8.0. Temperature is shown at the bottom graph by the red line while the y-axis ranges from 0 to 20. The x-axis for both current constant and future constant are the dates that range from July 26, 2023, to August 4, 2023. The right side set of graphs represents the performance for future constant. The dashed blue lines are the programmed set points for future constant conditions. Oxygen is shown at the top by the yellow line and the y-axis range is from 0 to 10. The pH is in the middle graphs from top to bottom and is shown by the pink line with a y-axis range of 6.5 to 8. Finally, the temperature is at the bottom shown by a red line and a y-axis range of 0 to 20.

DISCUSSION

Based on our high mortality percentages our experimental design did not work. We did not have enough data to make concrete conclusions about the processes happening within each of our experimental treatments. We were only able to make qualitative observations about what was happening with the small amount of surviving red abalone larvae. For example, an important observation that was made was that by day 3 of the experiment, the two future conditions had a

higher developmental score compared to the current conditions. Both future variables and future constant had their larvae develop up to the N stage while current constant and current variable only had their larvae reach the I stage. Looking closer at the different temperature set points for those four treatments, the future conditions had warmer environments than the current conditions. The average temperature for future conditions was 14.5℃ which is warmer than the average temperature for current conditions 11.5℃. Recalling Leighton's experiment of larval development based on temperature, we can justify that the reason why the larvae inoculated into the future experimental conditions developed quicker was because of the warmer temperatures.

Red abalone larvae develop slower at lower temperatures and quicker at their own desirable temperatures, if the temperature is too hot then development stops and the larvae die (Leighton, 1974). We started to lose that observation by day 6 due to the fact that there were not many larvae to compare to each other. Our survival percentage at day 6 was 98% which did not give us enough information to make assumptions about development. The best subset that we were able to use were the few samples from day 3 that were sorted. From there we confirmed that larval development is based on temperature when looking at Leighton's work and examining that at day three a larvae being reared at temperatures around 11.5℃ will be able to reach the "cap-shell veliger" stage which is equivalent to the G/H stage observed within our current experimental treatments (Fig 12). Our data along with Leighton's also shows that larvae that are reared in 14.5℃ tend to be at the "operculate veliger" stage by day 3, which is equivalent to the N stage that was observed within our future experimental treatments at day 3 (Fig 12).

In terms of pH and DO we cannot make any correlations because of how the upwelling system performed and was unable to accurately meet the programmed set points for DO and pH. The key piece of information extracted from our experiment was that development is temperature dependent and it correlates with previous studies and guidelines that the aquaculture industry uses. There are several factors that potentially contributed to our low survivorship such as poor husbandry, before and during the experiment, upwelling system performance, and other experimental designs such as our chambers.
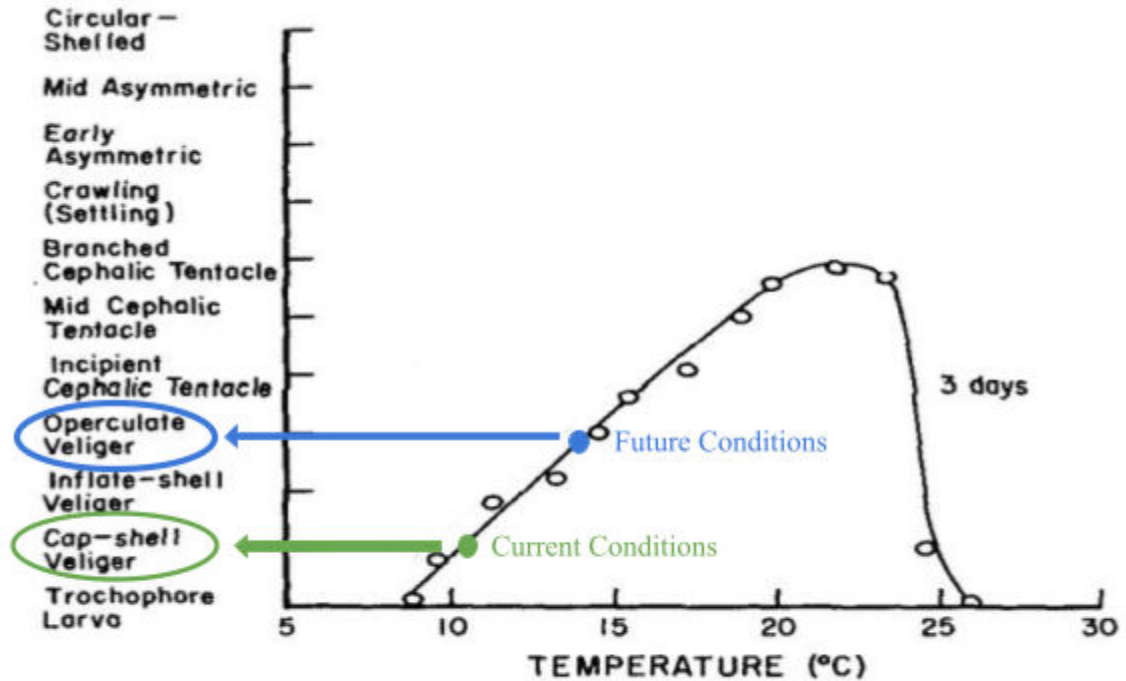
FIGURE 4.—Development of larvae of *Haliotis rufescens* at a series of temperatures when introduced to the thermal gradient as trochophores.

Figure 12: This graph is from Leighton's study on The influence of temperature on larval and juvenile growth in three species of southern California abalones. It shows the different developmental stages of red abalone on the y-axis going from early larval life stages at the bottom to late larval life stages at the top. The x-axis shows the temperatures in which the abalone are reared and the curve represents the development at day 3 depending on the temperature in which they are reared. The green circle highlights the "cap-shell veliger" stage which our current conditions were able to reach by day three when our average temperature was 11.5 ℃. The blue circle highlights the "operculate veliger" stage which our future conditions were able to reach by day three when our average temperature was 14.5 ℃.

CONCLUSION/RECOMMENDATIONS

There are multiple probable causes for our high mortality percentage that we failed to mitigate throughout our experiment. Some of these factors could have been our husbandry techniques before and during our experiment. Suggestions for future experiments like these include washing and thoroughly disinfecting everything in the upwelling system set up to prevent algae buildup or foreign debris from entering into the experimental chambers or clogging the water delivery system. We made an effort to sanitize everything we used during the

experiment, but we were unsure if the upwelling system needed more cleansing before starting the experiment. Changing the chamber design to fit a different inflow model could be helpful as we were unsure if having water flowing in from the top was causing impingement. The water inflow could be made at the bottom of the chamber to prevent impingement or we could follow the passive diffusion style used for ctenophores and other pelagic marine invertebrates at the Monterey Bay Aquarium (Patry et al. 2020).

Having a control treatment could be more insightful for future studies as well. With our experimental design, we did not include a control treatment that could be tailored for the successful survivorship and development of red abalone. For future experiments having a control treatment using the guidelines that the aquaculture industry uses to promote high survivorship can be informative. If those larvae survive and develop successfully, we can potentially rule out the idea of our experimental infrastructure being the cause of high mortality rates and slower development. Overall our experiment was headed in the right direction, but it needed more tailoring and more time to both conceptualize the experiment and analyze the samples thoroughly.

REFERENCES

Bakun A.(1990). Global Climate Change and Intensification of Coastal Ocean Upwelling. Science. 247(4939):198-201. https://www.jstor.org/stable/2873492

Bary JP, GravesD, Kecy C, Lovera C, Okuda C, Boch CA, Lord JP. (2017). Chasing the Future How Will Ocean Change Affect Marine Life? Oceanography. 30(4):60-7. https://www.jstor.org/stable/26367626.

Boch CA, Litvin SY, Micheli F, De Leo G, Aalto EA, Lovera C, Brock Woodson C, Monismith S, Barry JP. (2017). Effects of current and future coastal upwelling conditions on the fertilization success of the red abalone (Haliotis rufescens). Fields DM, editor. ICES Journal of Marine Science. 74(4):1125–1134. doi:https://doi.org/10.1093/icesjms/fsx017. https://academic.oup.com/icesjms/article/74/4/1125/3094691.

Booth, J. Ashley Tomer, "Hypoxic and low pH water in the nearshore marine environments of Monterey Bay, California: characterizing a decade of oxygen and pH, and drivers of variability" (2011). Capstone Projects and Master's Theses. 62.

Bryne, M., Ho, M., Wong, E., Soars, N. A., Selvakumaraswamy, P., Shepard-Brennand, H., Dworjanyn, S. A., & Davis, A. R. (2011). Unshelled abalone and corrupted urchins: development of marine calcifiers in a changing ocean. Proceedings. Biological sciences, 278(1716), 2376-2383. https://doi.org/10.1098/rspb.2010.2404

Crim RN, Sunday JM, Harley CDG. (2011). Elevated seawater CO_2 concentrations impair larval development and reduce larval survival in endangered northern abalone (Haliotis kamtschatkana). Journal of Experimental Marine Biology and Ecology. 400(1-2):272–277. doi:https://doi.org/10.1016/j.jembe.2011.02.002.

Hanh, K. O. (1989). Handbook of culture of abalone and other marine gastropods. CRC Press.

Leighton, David. (1974). The influence of temperature on larval and juvenile growth in three species of Southern California abalones. U.S. Department of Commerce, Fishery Bulletin. 72.

Lourenço CR, Nicastro KR, McQuaid CD, Lilian Anne Krug, Zardi GI. (2020). Strong upwelling conditions drive differences in species abundance and community composition along the Atlantic coasts of Morocco and Western Sahara. Marine Biodiversity. 50(2). doi:https://doi.org/10.1007/s12526-019-01032-z.

National Oceanic and Atmospheric Administration. Abalone Restoration and Management in Southern California. [accessed 2023 Jul 17]. https://www.fisheries.noaa.gov/s3/dam-migration/noaa_abalone_recovery_fact_sheet.pdf.

Patry WL, Bubel M, Hansen C, Knowles T. (2020). Diffusion tubes: a method for the mass culture of ctenophores and other pelagic marine invertebrates. PeerJ. 8:e8938. doi:https://doi.org/10.7717/peerj.8938.

Reum JCP, Alin SR, Harvey CJ, Bednaršek N, Evans W, Feely RA, Hales B, Lucey N, Mathis JT, McElhany P, et al. (2015). Interpretation and design of ocean acidification experiments in upwelling systems in the context of carbonate chemistry co-variation with temperature and oxygen. ICES Journal of Marine Science. 73(3):582–595. doi:https://doi.org/10.1093/icesjms/fsu231.

Somero GN, Beers JM, Chan F, Hill TM, Klinger T, Litvin SY. (2015). What Changes in the Carbonate System, Oxygen, and Temperature Portend for the Northeastern Pacific Ocean: A Physiological Perspective. BioScience. 66(1):14–26. doi:https://doi.org/10.1093/biosci/biv162.